# Electronic Supplementary Material

# Engineering the electronic and geometric structure of $VO_x$/BN@$TiO_2$ heterostructure for efficient aerobic oxidative desulfurization

Lu Zhang[1], Jixing Liu (✉)[1], Deqi Huang[2], Wenfeng Zhang[1], Linjie Lu[1], Mingqing Hua[1], Hui Liu[1], Huifang Cheng[1], Huaming Li[1], Wenshuai Zhu (✉)[1]

1 School of Chemistry and Chemical Engineering, Institution for Energy Research, Jiangsu University, Zhenjiang 212013, China

2 College of Chemical Engineering, Yangzhou Polytechnic Institute, Yangzhou 225127, China

E-mails: jxliu0804@ujs.edu.cn (Liu J); zhuws@ujs.edu.cn (Zhu W)

### *1. Catalyst Characterization*

X-ray powder diffraction (XRD) was performed on a Shimadzu XRD-6100 Lab X-ray diffractometer with Cu Kα radiation. Transmission electron microscopy (TEM) images were collected on a JEOL-JEM-2010 transmission electron microscopy (TEM, JEOL-JEM-2010) with an operating voltage of 200 kV and a JEOL JSM-7001F with an operating voltage of 15 kV. X-ray photoelectron spectroscopy (XPS) was performed on a ESCALAB 250Xi (USA) analyzer. The reducibility of catalyst was characterized by temperature-programmed reduction with hydrogen ($H_2$-TPR). Gas chromatography-mass spectrometry (GC-MS) was applied for the detection of oxidative product and the discussion of mechanism in diesel with analyzer Agilent 7890/5975C (USA). Electron

spin resonance (ESR) spectra were conducted by a JES FA200 spectrometer at ambient temperature.

### *2. Turnover frequency (TOF)*

Turnover frequency (TOF) was defined as the moles of sulfur containing molecules converted by the moles of V atoms in the catalysts per second.

$$\mathrm{TOF}=\frac{\eta\times \mathrm{Sulfur(mol)}}{n_{\mathrm{V\text{-}surf}}(\mathrm{mol})\times \mathrm{Time(s)}} \quad (1)$$

Where, TOF was calculated with the $\eta$ < 20% under the exclusion of interparticle mass-transfer limitation. Also, $n_{V\text{-}surf}$ is the mole number of V atoms on the surfaces of catalysts (mol), which was estimated based on the XPS and BET data.

$$n_{V\text{-}surf} = \frac{N_{V\text{-}surf}}{N_A} \quad (2)$$

Where $n_{v\text{-}surf}$ is the number of V atoms on the surfaces of catalysts and $N_A$ is the Avogadro constant ($6.02\times10^{23}$ $mol^{-1}$)

The calculation formulas of $N_{v\text{-}surf}$ as follows:

$$\begin{aligned} m_{catal}\cdot S_{surf} &= S_{Ti\text{-}surf}+S_{B\text{-}surf}+S_{N\text{-}surf}+S_{V\text{-}surf}+S_{O\text{-}surf} \\ &= N_{Ti\text{-}surf}\cdot S_{Ti\text{-}single}+N_{B\text{-}surf}\cdot S_{B\text{-}single}+N_{N\text{-}surf}\cdot S_{N\text{-}single} \\ &\quad + N_{V\text{-}surf}\cdot S_{V\text{-}single}+N_{O\text{-}surf}\cdot S_{O\text{-}single} \end{aligned} \quad (3)$$

Where $S_{V\text{-}single}$ ($m^2$), $S_{Ti\text{-}single}$ ($m^2$), $S_{O\text{-}single}$ ($m^2$), $S_{B\text{-}single}$ ($m^2$), and $S_{N\text{-}single}$ ($m^2$), are the surface areas of single atoms, which were estimated by the hemispheric surface area ($2\pi r^2$), $S_{surf}$ ($m^2\cdot g^{-1}$) stands for the specific surface area of catalysts and $m_{catal}$ (g) represents the mass of catalysts (0.02 g).

The atomic radii employed for V, Ti, O, B, and N are shown as follows: $r_V = 1.34\times10^{-10}$ m, $r_{Ti} = 1.47\times10^{-10}$ m, $r_O = 6.40\times10^{-11}$ m, $r_B = 9.00\times10^{-11}$ m, and $r_N = 8.00\times10^{-11}$ m. The relationship between $N_{V\text{-}surf}$, $N_{Ti\text{-}surf}$, $N_{O\text{-}surf}$, $N_{B\text{-}surf}$, and $N_{N\text{-}surf}$ was calculated based on XPS (**Table 1** shows Normalized ratio of each element calculated by using XPS).

**Table S1** Textural properties of $VO_x/BNNS@TiO_2$ catalysts.

| Samples | $S_{BET}$ ($m^2\cdot g^{-1}$) | $V_p$ ($cm^3\cdot g^{-1}$) |
|---|---|---|
| $VO_x/TiO_2$ | 24.5 | 0.013 |
| $VO_x$/BNNS | 25.5 | 0.013 |
| $VO_x$/BNNS@$TiO_2$-1 | 24.2 | 0.013 |
| $VO_x$/BNNS@$TiO_2$-2 | 22.6 | 0.012 |
| $VO_x$/BNNS@$TiO_2$-3 | 22.8 | 0.012 |

**Table S2** Correlation fitted data of O 1s XPS and area ratios for $VO_x$/BNNS@$TiO_2$ catalysts.

| Sample | Fitted area | | | area ratios |
|---|---|---|---|---|
| | $O_\alpha$ | $O_\beta$ | O | $O_\beta$/O |
| $VO_x$/BNNS | 76672.1 | 5564.0 | 82236.1 | 0.07 |
| $VO_x$/BNNS@$TiO_2$-1 | 32308.9 | 18273.2 | 50582.2 | 0.36 |
| $VO_x$/BNNS@$TiO_2$-2 | 43486.1 | 56096.0 | 99582.1 | 0.56 |
| $VO_x$/BNNS@$TiO_2$-3 | 45215.2 | 67098.6 | 112313.8 | 0.60 |

**Table S3** Correlation fitted data of V $2p_{3/2}$ XPS and area ratios for $VO_x$/BNNS@$TiO_2$ catalysts.

| Sample | Fitted area | | area ratios |
|---|---|---|---|
| | $V^{5+}$ | $V^{4+}$ | $V^{5+}$/ $V^{4+}$ |
| $VO_x$/BNNS | 1142.5 | 1132.2 | 1.01 |
| $VO_x$/BNNS@$TiO_2$-1 | 3707.7 | 3300.2 | 1.12 |
| $VO_x$/BNNS@$TiO_2$-2 | 8265.1 | 5704.8 | 1.45 |
| $VO_x$/BNNS@$TiO_2$-3 | 8243.2 | 6759.3 | 1.22 |

**Table S4**. Comparison of catalytic ODS activities of $VO_x$/BNNS@$TiO_2$-2 with recently reported Mo/W/V-Containing catalysts.

| Entry | Catalyst | Oxidant | Substrate | Reaction temperature | Reaction conditions | TOF ($s^{-1}$) | Ref. |
|---|---|---|---|---|---|---|---|
| 1 | Mn-Mo-O | air | DBT | 110 ℃ | 500 ppm, catalyst dosage 0.5 $g{\cdot}L^{-1}$ | $1.23\times10^{-3}$ | [1] |
| 2 | $TiO_2/SiO_2$ | TBHP | DBT | 80 ℃ | 500 ppm, catalyst dosage 10 $g{\cdot}L^{-1}$ | $6.83\times10^{-3}$ | [2] |
| 3 | Co-Pc/PMoV | $O_2$ | DBT | 100 ℃ | 500 ppm, catalyst dosage 2 $g{\cdot}L^{-1}$ | $0.68\times10^{-2}$ | [3] |
| 4 | Co-Fe-Mo-MMO-2 | $O_2$ | DBT | 100 ℃ | 500 ppm, catalyst dosage 1 $g{\cdot}L^{-1}$ | $0.63\times10^{-3}$ | [4] |
| 5 | Co-Mo-O | air | DBT | 100 ℃ | 500 ppm, catalyst dosage 1 $g{\cdot}L^{-1}$ | $0.73\times10^{-3}$ | [5] |
| 6 | (Cu-Co)salenY | $O_2$ | DBT | 80 ℃ | 500 ppm, catalyst dosage 8 $g{\cdot}L^{-1}$ | $3.37\times10^{-3}$ | [6] |
| 7 | $Cr_2WO_6$/$WO_3$ | $H_2O_2$ | DBT | 70 ℃ | 870 ppm, catalyst dosage 5 $g{\cdot}L^{-1}$ | $0.52\times10^{-3}$ | [7] |
| 8 | CuO/$SiO_2$@V-PIL | $O_2$ | DBT | 120 ℃ | 500 ppm, catalyst dosage 5 $g{\cdot}L^{-1}$ | $5.61\times10^{-6}$ | [8] |
| 9 | $MoO_3/Al_2O_3$ | $H_2O_2$ | DBT | 75 ℃ | 320 ppm, catalyst dosage 1.3 $g{\cdot}L^{-1}$ | $0.19\times10^{-2}$ | [9] |
| 10 | $VO_x$/BNNS@$TiO_2$-2 | $O_2$ | DBT | 130 ℃ | 200 ppm, catalyst dosage 1 $g{\cdot}L^{-1}$ | $4.80\times10^{-2}$ | This work |

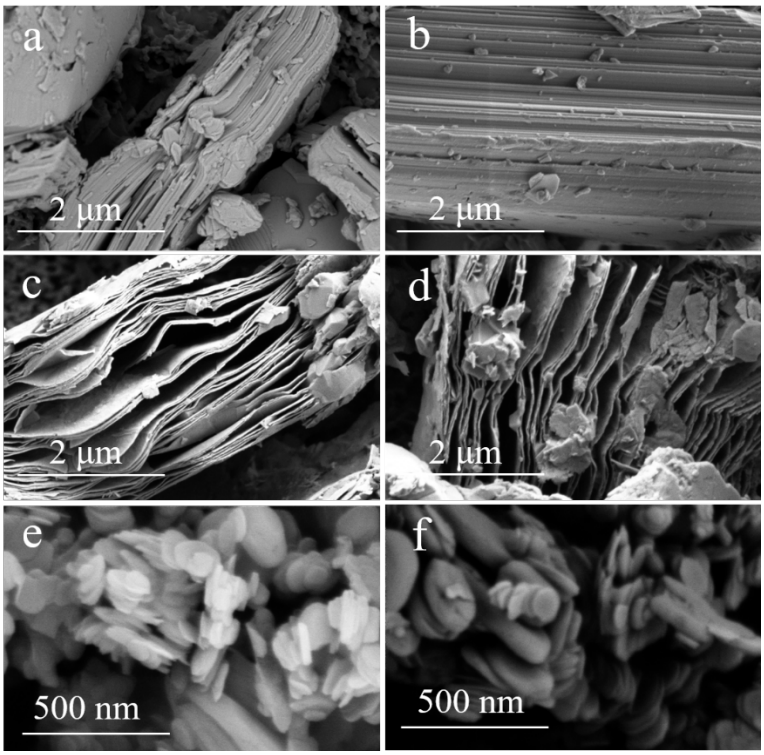


**Fig. S1**. SEM images of the catalysts: (a, b) $Ti_3AlC_2$ MAX; (c, d) $Ti_3C_2$ MXene; (e, f) BNNS.

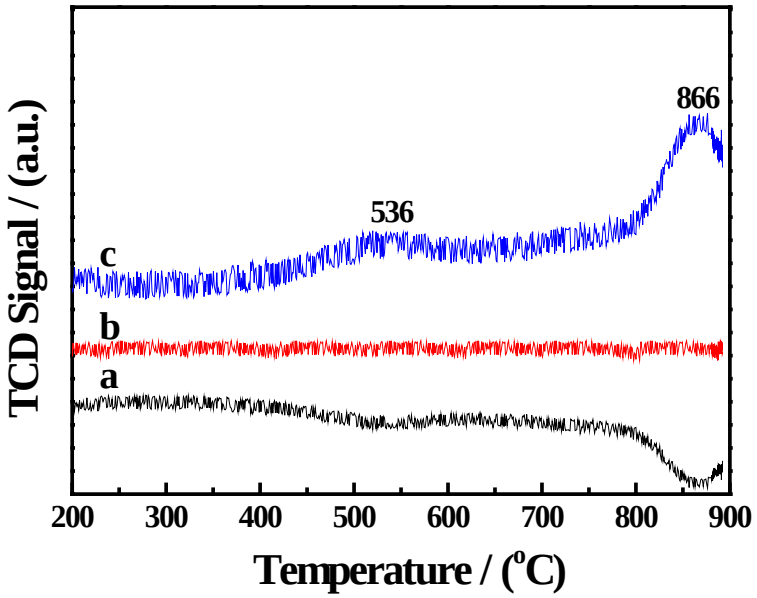


**Fig. S2**. $H_2$-TPR profile of the catalysts: (a) BNNS, (b) $TiO_2$, (c) $VO_x/TiO_2$.

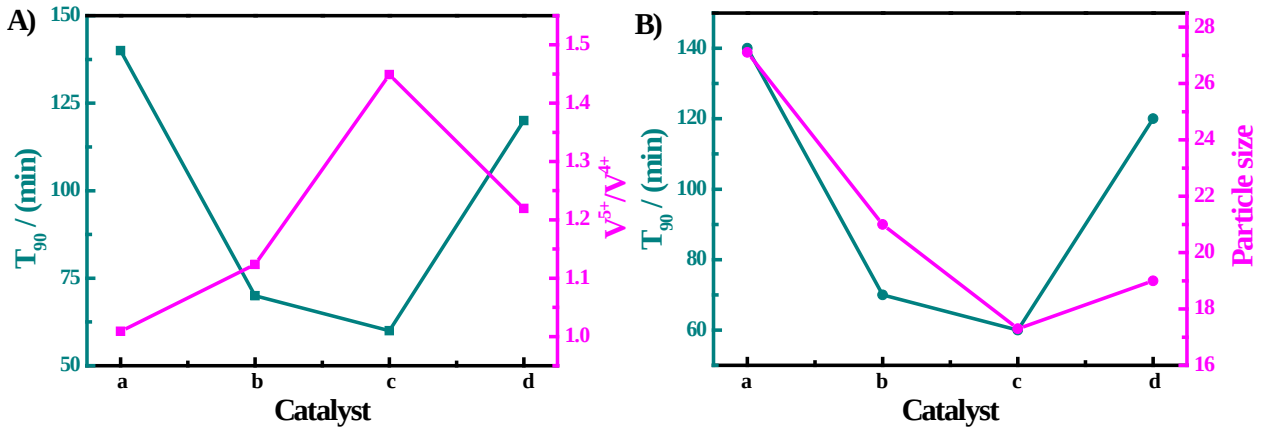


**Fig. S3.** Comparison of time required for different catalysts to achieve 90% conversion with (A) $V^{5+}/V^{4+}$ (B) particle size of these catalysts: (a) $VO_x$/BNNS (b) $VO_x$/BNNS@$TiO_2$-1 (c) $VO_x$/BNNS@$TiO_2$-2 (d) $VO_x$/BNNS@$TiO_2$-3.

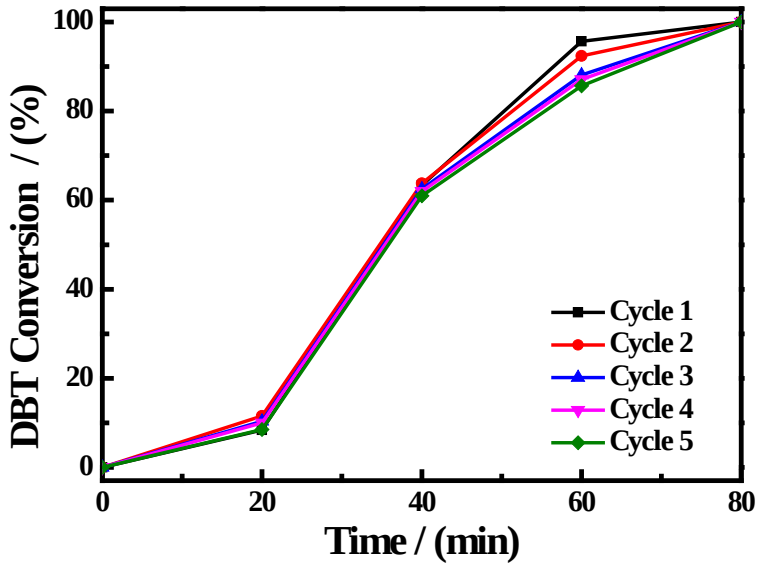


**Fig. S4.** Catalytic stability of the representative $VO_x$/BNNS@$TiO_2$-2 sample in ODS system.

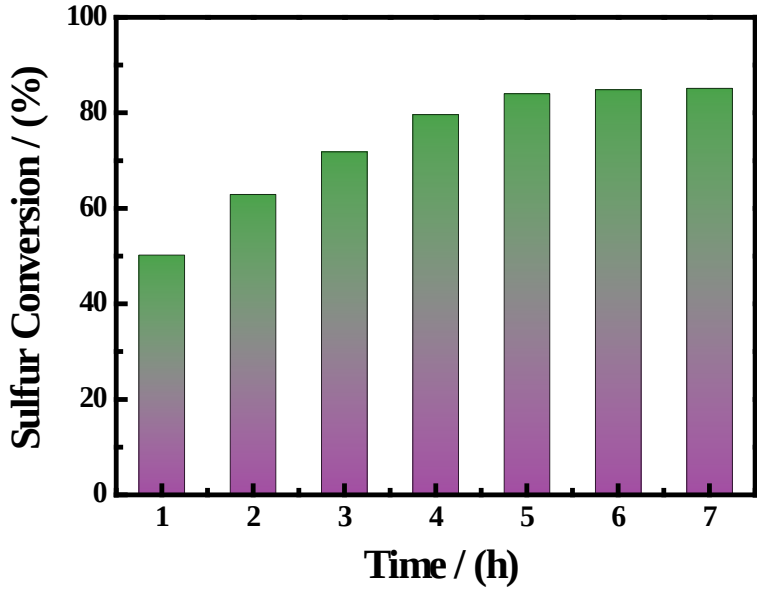


**Fig. S5.** The sulfur conversion for real diesel over $VO_x$/BNNS@$TiO_2$-2. Experimental conditions: v($O_2$) = 200 mL·$min^{-1}$, T = 130 ℃, V(oil) = 20 mL, r = 800 rpm and m(catalyst) = 0.02 g.
X

## References

1. Bai J, Song Y, Wang C, Chen H, Wei D, Bai L,Wang W, Yang L, Liang Y, Yang H. Engineering the electronic structure of Mo sites in Mn-Mo-O mixed-metal oxides for efficient aerobic oxidative desulfurization. Energy & Fuels, 2021, 35(15): 12310-12318
2. Bazyaria A, Khodadadia A, Mamaghania A, Beheshtianb J, Thompsonc L, Mortazavia Y. Microporous titania-silica nanocomposite catalyst-adsorbent for ultra-deep oxidative desulfurization. Applied Catalysis B: Environmental, 2016, 180: 65-77
3. Li Y, Zhang H, Jiang Y, Shi M, Bawa M, Wang X, Zhu S. Assembly of metallophthalocyanine-polyoxometalate hybrid for highly efficient desulfurization of organic and inorganic sulfur under aerobic conditions. Fuel, 2019, 241: 861-869
4. Song Y, Bai J, Jiang S, Yang H, Yang L, Wei D, Bai L, Wang W, Liang Y, Chen Y. Co-Fe-Mo mixed metal oxides derived from layered double hydroxides for deep aerobic oxidative desulfurization. Fuel, 2021, 306: 121751
5. Dong Y, Zhang J, Ma Z, Xu H, Yang H, Yang L, Bai L, Wei D, Wang W, Chen H. Preparation of Co-Mo-O ultrathin nanosheets with outstanding catalytic performance in aerobic oxidative desulfurization. Chemical Communications, 2019, 55(93): 13995-13998

6. Yu J, Zhu Z, Ding Q, Zhang Y, Wu X, Sun L, Du J. Oxidative desulfurization of dibenzothiophene with molecular oxygen using cobalt and copper salen complexes encapsulated in NaY zeolite. Catalysis Today, 2020, 339: 105-112
7. Wang H, Tang M, Shi F, Ding R, Wang L, Wu J, Li X, Liu Z, Lv B. Amorphous $Cr_2WO_6$-modified $WO_3$ nanowires with a large specific surface area and rich lewis acid sites: a highly efficient catalyst for oxidative desulfurization. ACS Applied Material Interfaces, 2020,12(34): 38140-38152
8. Li A, Song H, Meng H, Lu Y, Li C. Peroxovanadic based core-shell bifunctional poly(ionic liquid)s catalyst $CuO/SiO_2$@V-PIL: its in-situ free radical initiation mechanism for air oxidative desulfurization. Fuel, 2022, 310: 122430
9. Safa M A, Ma X. Oxidation kinetics of dibenzothiophenes using cumene hydroperoxide as an oxidant over $MoO_3/Al_2O_3$ catalyst. Fuel, 2016, 171: 238-246